

1    **Title**

2    **Transboundary hotspots associated with SARS-like coronavirus**  
3    **spillover risk: implications for mitigation**

4    **Authors**

5    *Renata L. Muylaert<sup>1\*</sup>, David A Wilkinson<sup>2</sup>, Tigga Kingston<sup>3</sup>, Paolo D’Odorico<sup>4</sup>, Maria Cristina Rulli<sup>4</sup>,*  
6    *Nikolas Galli<sup>4</sup>, Reju Sam John<sup>1</sup>, Phillip Alviola<sup>6</sup>, David T. S. Hayman<sup>1</sup>*

7    **Affiliations**

8    <sup>1</sup> *Massey University, Palmerston North, New Zealand*

9    <sup>2</sup> *Université de La Réunion, UMR Processus infectieux en milieu insulaire tropical (PIMIT) CNRS 9192, INSERM 1187, IRD 249, Sainte-*  
10    *Clotilde, La Réunion, France*

11    <sup>3</sup> *Department of Biological Sciences, Texas Tech University, Lubbock, TX, U.S.A.*

12    <sup>4</sup> *Department of Environmental Science, Policy, and Management, University of California, Berkeley, Berkeley, CA, U.S.A.*

13    <sup>5</sup> *Department of Civil and Environmental Engineering, Politecnico di Milano, Milan, Italy*

14    <sup>6</sup> *Institute of Biological Sciences, University of the Philippines- Los Banos, Laguna, Philippines*

15    \*Corresponding author: [R.deLaraMuylaert@massey.ac.nz](mailto:R.deLaraMuylaert@massey.ac.nz)

16    **Abstract:** The emergence of SARS-like coronaviruses is a multi-stage process from wildlife  
17    reservoirs to people. Here we characterize multivariate indicators associated with the risk of zoonotic  
18    spillover of SARS-like coronaviruses in different areas to help inform surveillance and mitigation  
19    activities. We consider direct and indirect transmission pathways by modeling four scenarios with  
20    livestock and mammalian wildlife as potential and known reservoirs, before examining how access to  
21    healthcare varies within areas. We found 19 multivariate clusters that had differing risk factor  
22    contributions. High-risk areas were mostly close (11-20%) rather than far (<1%) from healthcare.  
23    With the presented framework, areas with the highest estimated risk can be priority intervention  
24    targets in which risk management strategies can be implemented, such as land use planning and  
25    preventive measures to reduce contact between people and potential hosts.

26    **Key-words:** zoonotic risk, viral emergence, land conversion, deforestation, host diversity,  
27    coronavirus, pandemics, sarbecovirus, One Health, scenario analysis

28  
29    **Teaser:** Multivariate clusters of stressors associated with SARS-like coronavirus spillover risk.

## 30      **Introduction**

31      Human infectious diseases almost all came from other species (1). COVID-19, Ebola virus disease,  
32      HIV/AIDS and Zika virus disease are recent examples, whereas those like measles arose after the  
33      Neolithic Agricultural Revolution (2). The process of infectious disease emergence from animals  
34      begins with the cross-species transmission (spillover) of a microbe (e.g., virus, bacteria, fungus) to a  
35      new animal host in which it is pathogenic (1, 3, 4). Yet, successful emergence events are complex  
36      multi-stage processes with many possible pathways leading from the original wildlife reservoir to  
37      sustained transmission in people (5). The probability of any of these pathways occurring and resulting  
38      in infection emergence varies temporally and spatially. Understanding where and why viruses  
39      spillover is essential to prevent future pandemics. Pervasive, accelerated land use change (6), human  
40      encroachment, increasing and changing contacts among and between wildlife and domestic animals  
41      are among the multiple drivers of zoonotic pathogen transmission (7). However, the exact pathways  
42      of disease emergence are often unclear (8, 9). Cross-scale evaluation of disease emergence drivers,  
43      that can be measured and mapped, may allow decision-makers to know where to act and implement  
44      surveillance (10). Thus, effective risk evaluations must consider a variety of land use drivers as well  
45      as trends in the distribution of human and animal populations to optimally identify areas of change to  
46      focus mitigation measures (reduce pressures) and surveillance (11).

47      Zoonotic disease risk has been mostly linked to mammals and birds (12). Bats are among the  
48      natural hosts of viruses in the coronavirus (family *Coronaviridae*) subgenus *Sarbecovirus* (Severe  
49      acute respiratory syndrome (SARS)-related coronaviruses), that includes SARS-CoV-1 and SARS-  
50      CoV-2 (13, 14). Bat hosts of sarbecoviruses are broadly distributed but the highest diversity is in  
51      Southeast Asia (15). Human infection with *Sarbecovirus* from bats may be more frequent than  
52      reported from traditional surveillance (16) and potentially secondary hosts (17, 18). Viral infection  
53      prevalence contributes to the risk of spillover (4), and can be influenced by biological factors such as  
54      birthing cycles (19, 20) and external stimuli such as human changes to land use (7) (but see (21, 22)).

55      Large scale risk assessments in which areas with similar risk profiles are identified provide  
56      invaluable information (13, 23) and can be rapid, while the development of local, detailed and  
57      intricate spillover and outbreak risk assessments can take a long time (24, 25). Since detailed and  
58      validated data for recent reports on outbreak risk reduction are lacking for most regions of the globe  
59      (e.g. the Sendai framework, <https://sendaimonitor.undrr.org/>), a broad evaluation targeting  
60      *Sarbecovirus* emergence can be advantageous to discuss diverse contexts across the region where  
61      most natural hosts of sarbecoviruses occur. Human encroachment has led to decreased distances  
62      between bat roosts and human settlements (26), so part of the relevant hazard for inferring spillover  
63      risk can be spatially quantified from remotely sensed proxies for socioecological risk factors. Previous

64 works estimated host distributions (15, 27) and developed modeling frameworks for adding proxies  
65 for disease risk and spread in the face of limited data (15, 27, 28).

66 Here, we identify where indicators for emergence risk overlap, focusing on the biological  
67 possibility of the emergence of a *Sarbecovirus*. Our goal is to aid mitigation and surveillance  
68 activities throughout South, East and Southeast Asia, by identifying both where efforts should focus  
69 and which risk factors should be prioritized. Specifically, we aim to: 1) Identify and characterize  
70 univariate hotspots for four suggested spillover scenarios. 2) Identify spatially cohesive clusters of all  
71 risk indicators that, when combined, increase risk of zoonotic spillover (23, 29); 3) Quantify  
72 intersections of high-risk areas and access to health care, to identify where infection may be first  
73 detected and outbreaks may spread.

74 The four scenarios evaluated represent different nested transmission pathways. We assume  
75 that the risk of emerging new SARS-like outbreaks is associated with social, biological and  
76 environmental components and, because there are unobserved dynamics for emerging viruses (30), we  
77 evaluated four nested spillover pathway scenarios based on landscape change and potential hosts (31):  
78 Scenario 1 (direct - known bat hosts) represents direct transmission from bats to people, facilitated by  
79 the landscape condition, human population, and known bat hosts. Although molecular investigations  
80 suggest that direct transmission of sarbecoviruses from bats to humans may be possible (32), it has yet  
81 to be better documented (33). Rather, the involvement of an intermediary or bridging host appears  
82 more likely, perhaps because this allows for recombination and viral evolution, and/or leads to greater  
83 exposure to human populations. Consequently, we developed Scenarios 2-4 to represent indirect  
84 pathways that build on Scenario 1 by adding livestock (Scenario 2, indirect - mammalian livestock)  
85 and wild mammals (Scenario 3, indirect - wild mammals). Scenario 4 (indirect - all mammals) is a  
86 global scenario comprising landscape condition, human population, known bat hosts, mammalian  
87 livestock and wild mammals.

## 88 **Results**

### 89 *Characterization of univariate risk indicator hotspots*

90 The study region comprises a 25796-pixel grid for the terrestrial area evaluated. Univariate hotspot  
91 areas differ in magnitude (Figure 1) and extent according to components/indicators. Most hotspots  
92 concentrate at latitudes between 20 and 40 degrees. The univariate hotspots with the largest spatial  
93 extent are those obtained for agricultural and harvest land, followed by high integrity forests and areas  
94 with high deforestation potential. The majority of the included region comprises coldspots for primary  
95 bat hosts. Indicators with the greatest extent of coldspots were livestock (pigs then cattle) followed by  
96 known bat hosts. The largest extent of intermediate areas was for human population counts, which

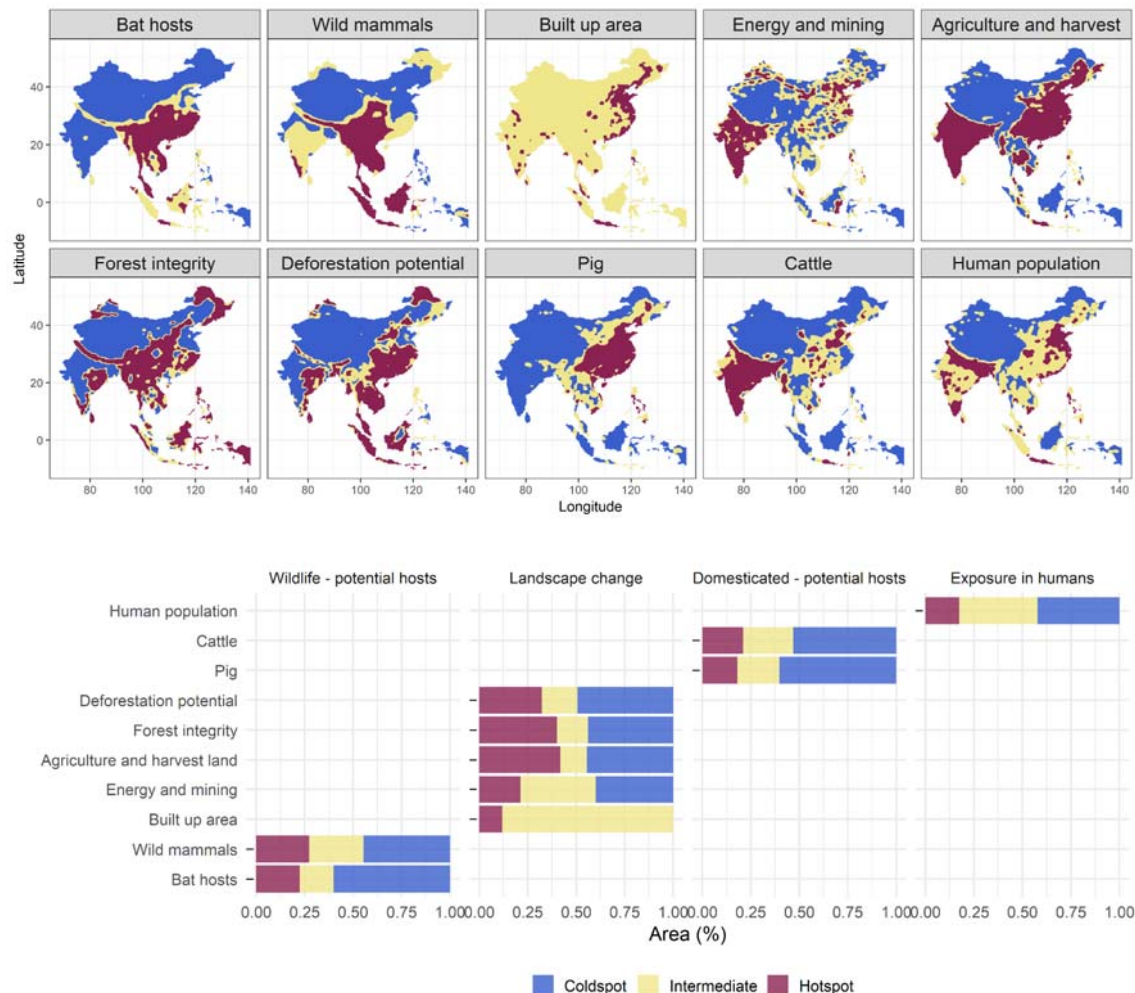
97 presented no coldspots due to the ubiquitous nature of human occupation in terrestrial areas. The  
98 largest differences in all Bovidae livestock versus cattle-only hotspots (see Methods) are in central  
99 China, parts of north (Hebei, Shanxi, and Henan) China and central India (Figure S2). The complete  
100 overlap of hotspots considering all univariate hotspots at one grid never occurred.

101

102

103

104



105

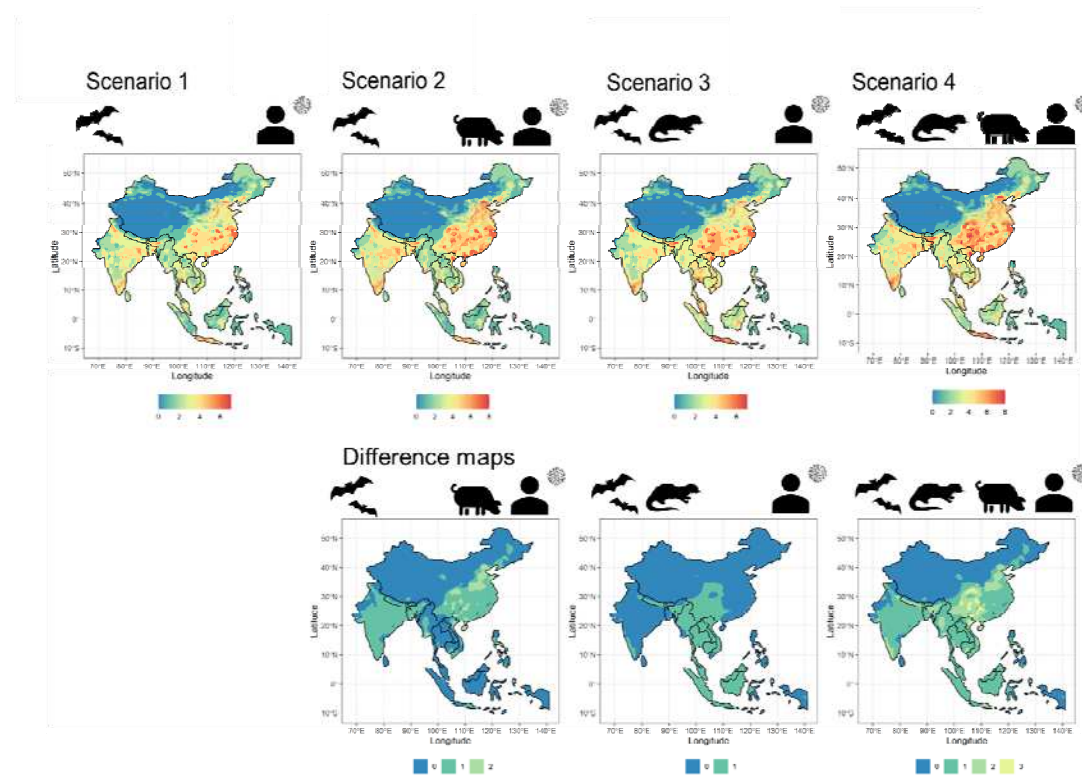
106 **Figure 1. Univariate hotspots of potential factors contributing to emergence of SARS-like**  
107 **coronaviruses.** The upper panel shows the spatial distribution of hotspots based on univariate  
108 indicators of risk of new *Sarbecovirus* emergence evaluated in four scenarios. Bottom panel shows the  
109 proportion (%) of areas classified as hotspots, intermediate or coldspots across the study region,  
110 according to the aggregation of indicators in higher-level groups and univariate descriptors. Areas in  
111 the red zone represent hotspots, yellow zones are intermediate areas and coldspots in blue, at a 95%  
112 alpha error level.

113

114 *Scenarios*

115 Regardless of scenario, the largest hotspot overlaps occur in central and southeast China, south and  
116 northwestern India and Java. Differences between Scenario 1 (direct - known bat hosts) with potential  
117 primary known bat hosts and Scenario 4 (indirect - all mammals) are largest in central China (Figure  
118 2). The largest differences between each scenario and Scenario 1 (the scenario with fewest covariates)  
119 concentrated in central and southern China and represent the hotspots from the variables that were left  
120 out in the difference maps. Scenario 3 was the one with the least amount of differences in relation to  
121 Scenario 1. Similar to Scenario 1, Scenario 2 shows most hotspot convergences in central and south  
122 China. Considering Scenario 4 (indirect - all mammals), the most important PCA axes show a clear  
123 'natural axis' and an anthropogenic axis, where the pig production layer is intermediate to the  
124 influence of both axes (Figure S3). Both main axes explain 58.7% of the total variation (PC1 = 33.5%,  
125 PC2 = 24.8%).

126 Maximum overlap for non-human potential primary and secondary hosts occurred across China and  
127 Vietnam. The average time to reach healthcare in areas with complete overlap among potential non-  
128 human hosts in areas is 1.04 h (0.76 SD). The fastest travel to healthcare times occurred in hotspots  
129 for all host groups except wild mammals secondary hosts, where the fastest travel to healthcare times  
130 were associated with intermediate areas and not hotspots (Table 1).



131

132

**Figure 2. Multivariate emergent risk hotspots for scenarios containing indicators associated with landscape change and zoonotic pathogen emergence.** Landscape, human population and known bat hosts are included in all models, and are the sole indicators in Scenario 1, representing direct transmission. To incorporate indirect transmission through secondary hosts, mammalian livestock are included in Scenario 2, wild mammals in Scenario 3, and both mammalian livestock and wild mammals in Scenario 4. The bottom panel shows differences between each upper respective scenario and Scenario 1. The internal white area in the continent represents no data values for Lake Qinghai; the largest lake in China.

133

134

135

136

137

138

139

140

141

142

**Table 1. Average time to reach healthcare in areas with complete overlap for non-human potential hosts within China and Vietnam.** Wild mammal refers to wild mammals except for the known bat host species.

Time to reach healthcare (mean hours, [SD])

Component in potential transmission risk scenario	Coldspot	Intermediate	Hotspot
<b>Primary hosts (known bat hosts)</b>	5.81 [10.2]	1.98 [3]	<b>1.76 [2.37]</b>
<b>Secondary hosts (wild mammal)</b>	6.62 [11.2]	<b>1.97 [3.57]</b>	2.26 [3.03]
<b>Secondary hosts (pig)</b>	6.08 [10.2]	1.92 [2.83]	<b>0.8 [0.73]</b>

**Secondary hosts (cattle)** 6.98 [10.6] 1.51 [1.93] **0.64 [0.72]**

143

144 *Hotspot overlap in clusters*

145 The optimal number of multivariate spatial clusters is nine when 10% of the human population is used  
146 as a minimum bound variable and 19 for 5% of the human population. There is an incremental benefit  
147 reduction from adding clusters, from nineteen groups on (Figure S4). The clusters from the cut-off  
148 value of 5% are nested within the 10% clusters (Figure S5), and we present the clusters for 19 areas in  
149 the main text (Figure 3). From the 19 clusters, Beijing (cluster 19), Java (cluster 17), and Sichuan and  
150 Yuzhong District, Chongqing (cluster 16, Table 2) concentrate the highest hotspot scores. The clusters  
151 with highest scores were among the smaller clusters in geographical extent. Inner-West China (cluster  
152 1), South Lhasa and Arunachal Pradesh (cluster 15), and Philippines, Timor East, West Papua (cluster  
153 9) had the highest scores for coldspots. Areas with the highest scores for the Intermediate class were  
154 Assam, West Burma block, Steppe and Sri Lanka (cluster 2), followed by Southwest Indochina  
155 (cluster 11) and North India (cluster 14). Clusters with the all Bovidae livestock version are in Figure  
156 S6, and they were very similar to the cattle-only versions, except for the Beijing area and the division  
157 of the two larger clusters in India, West India and East India.

158

159 **Table 2. Multivariate spatial clusters and the number of times in which the median values of**  
160 **each emergent risk score were in coldspots, intermediate or hotspots (n=190).** The top three  
161 values for each column are in boldface.

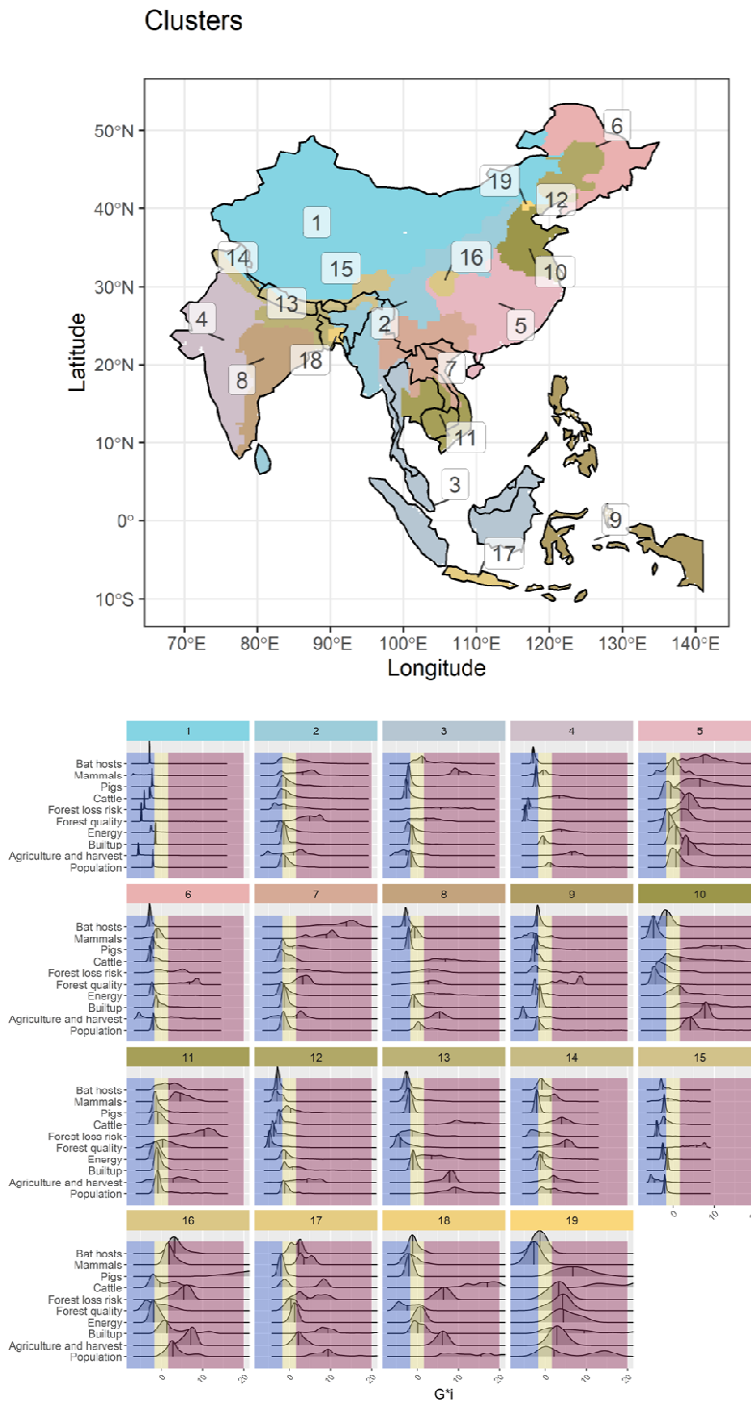
Cluster ID and indicative name N variables for which the median is a

	Coldspot	Intermediate	Hotspot
	spots		
<b>1 Inner-West China</b>	<b>9</b>	1	0
<b>2 Assam, West Burma block, Steppe, and Sri Lanka</b>	0	<b>8</b>	2
3 West Thailand, most of Sundaland islands	3	4	3

4 West India	4	3	3
5 Central China	0	5	5
6 Manchuria	6	3	1
7 North Lao PDR, North Vietnam, South China	0	5	5
8 East India	2	3	5
<b>9 Philippines, Timor East, West Papua</b>	<b>7</b>	2	1
10 North China	5	0	5
<b>11 Southwest Indochina</b>	0	<b>6</b>	4
12 Inner Manchuria	5	4	1
13 Nepal, Bhutan, Bangladesh	4	2	4
<b>14 North India</b>	1	<b>6</b>	3
<b>15 South Lhasa and Arunachal Pradesh</b>	<b>8</b>	1	1
<b>16 Sichuan and Yuzhong District, Chongqing</b>	2	2	<b>6</b>
<b>17 Java</b>	1	2	<b>7</b>
18 East Bangladesh	2	4	4
<b>19 Beijing</b>	1	1	<b>8</b>
<b>Total</b>	60	62	68

162

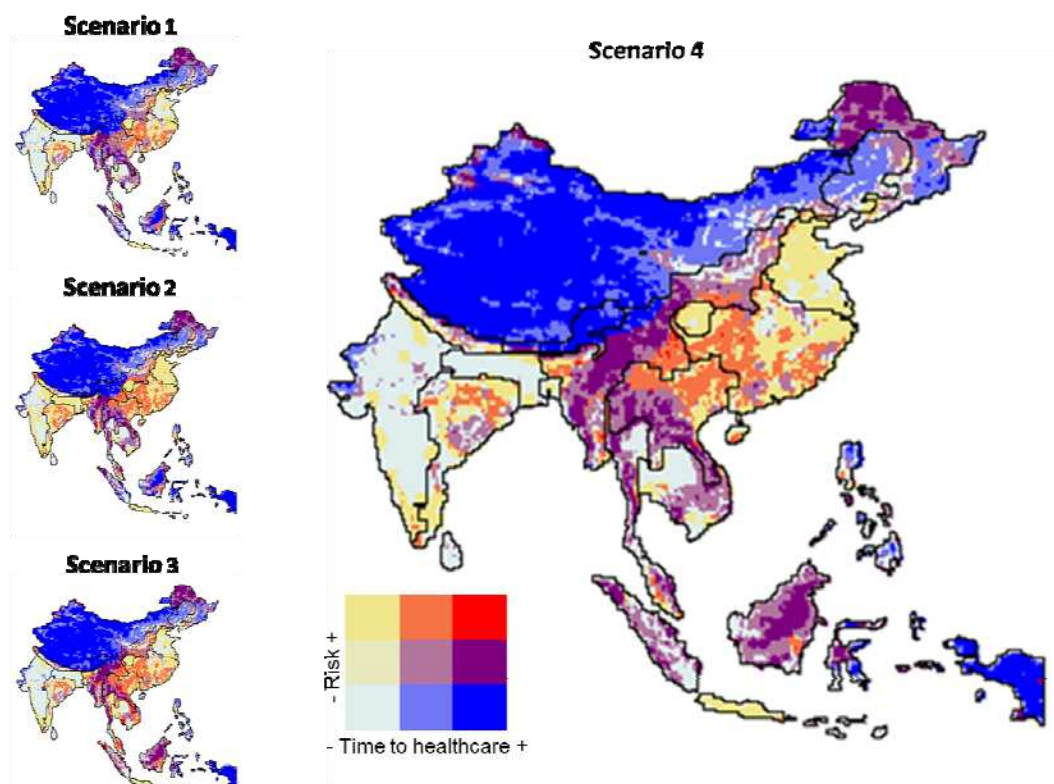
163



171 *Potential outbreak detection and spread*

172 When we cross the risk factor spatial information with healthcare access measured as travel time, the  
173 largest differences between combinations of quantiles of the two covariates are in the lowest and highest  
174 quantiles of both variables (Figure 4). We calculated the areas with high-risk values that are far or  
175 close to healthcare for all scenarios (Figure S7) within the spatial clusters from the skater analysis.  
176 From the entire study region, areas closer to healthcare that had high hotspot overlap (areas in yellow  
177 in Figure 4, Figure S7) covered an area ranging from 11.96% in Scenario 1, to 20.28% in Scenario 2,  
178 14.66% in Scenario 3, and 13.67% in Scenario 4. Areas far from healthcare that present high hotspot  
179 overlap (in red Figure 4 and Figure S7) were much rarer and varied according to scenarios, always  
180 covering less than 1% of the studied region, ranging from 0.1% in Scenario 1, to 0.30 in Scenario 2,  
181 0.91% in Scenario 3 and 0.22% in Scenario 4. The relationship between travel time to healthcare and  
182 human population counts (Figure S8) shows that areas far from healthcare tend to have lower  
183 population counts, but the relationship is non-linear.

184



185  
186 **Figure 4. Bivariate maps crossing emergent risk from hotspot data on risk quantiles and access**  
187 **to healthcare.** Black lines divide the limits for the 19 clusters identified.

188 **Discussion**

189       Urgent actions are needed to decrease disease emergence risk (34, 35). Using a macroscale  
190 approach, we assessed the distribution of locations with a greater risk of experiencing *Sarbecovirus*  
191 spillover events using landscape conditions and exposure of potential hosts (wildlife, domestic,  
192 human). Landscape conditions coupled with predictions of the distribution of known hosts and  
193 proxies for potential hosts and processes linked to human exposure to novel viruses can be a powerful  
194 tool for spatial sample prioritization when limited viral spillover information is available, such as for  
195 sarbecoviruses (16).

196       The overlap of risk factor hotspots represents pressure points on natural ecosystems that have  
197 been extensively altered in terms of agriculture, deforestation, and livestock production. In some  
198 cases, these clusters still have high values for forest quality and known host diversity (for instance,  
199 cluster 5 – central China, and cluster 17 – Java). Areas where outstanding values of different risk  
200 factors converge can pose a severe risk to disease emergence and conservation. In Sichuan – cluster  
201 16 – values of livestock production are extremely high and largely extensive farming takes place  
202 concomitantly with the presence of hotspots for mammal diversity (including higher values for known  
203 bat hosts) and very high deforestation risk. Unfortunately, deforestation rates and the livestock  
204 revolution are evident in our top-rated clusters (27), within biodiversity-rich areas, with high forest  
205 loss risk and a very large human population (in the case of Beijing - cluster 19 and Java - cluster 17).

206       We assume that intermediate areas in proximity to hotspots, and where socio-ecological  
207 transitions such as those related to the livestock revolution, are at the greatest risk of transitioning to  
208 hotspots (27). Even without transition, clusters with mostly intermediate values for stressors have had  
209 zoonotic spillovers in the past (17, 33, 36), notably those in central China on cluster 2 and edges with  
210 cluster 7 (north Lao PDR, north Vietnam, south China). Further, there is overlap of several identified  
211 clusters with areas that concentrate hosts of other viruses with pandemic potential, such as Nipah  
212 virus (37). The intermediate and high-risk areas within clusters need a multidimensional approach to  
213 mitigation that combines targeted surveillance of human populations and the highly weighted risk  
214 factors with One Health approaches. These approaches emphasise nature-based mitigation strategies,  
215 looking at the socio-economic drivers that shape local landscape conditions. Our analyses also show  
216 that risk factor clusters are commonly multinational, and action plans are a complex task to  
217 implement. However, transboundary, coordinated action between nations that share territorial limits is  
218 paramount if configuration of hotspots is taken into account when managing, protecting and restoring  
219 land to mitigate disease emergence risk.

220       Conditionally safer areas (blue, Figure 4) represent remote areas that present little spatial  
221 overlap in risk factor hotspots. In those areas, priority should be assessing and reducing other disaster  
222 and disease risks. In areas of high potential assessed risk (khaki, orange and red, Figure 4), actions

223 should be focused on the drivers of spillover. Recent literature (35) suggests three broad, cost-  
224 effective actions to minimize pandemic risk: better surveillance of pathogen spillover, better  
225 management of wildlife trade, and substantial reduction of deforestation (i.e. primary prevention)  
226 (35). Landscape planning should have priority, as these can have other benefits (38, 39) and can  
227 include preventive measures to reduce levels of contact between people and potential wild and  
228 domestic animal hosts. Biosecurity measures and surveillance and fauna monitoring are also key  
229 where multi-component risk levels are higher (40). Syndromic, virological, serological, and  
230 behavioral risk surveillance of people with regular proximity with known reservoir or potential  
231 amplifier hosts (40) can be of great value in these hotspots, but the ultimate prevention should be in  
232 primary prevention. Beyond viral monitoring and discovery, prevention can be achieved by reducing  
233 deforestation, wildlife trade and increasing sustainable management of agricultural areas (35).

234 Surveillance effort correlates with detecting infections and where human populations intersect  
235 with wildlife, risk increases (41, 42). Evidence from Brazil also suggests zoonotic risk increases with  
236 remoteness (along with increased wild mammal species richness) and decreases in areas with greater  
237 native forest cover (43). Our results suggest high-risk areas are often (11-20%) associated with faster  
238 travel times to healthcare, compared to remote areas (<1%) (yellow and red respectively, Figure 4).  
239 The problem posed by remote sites for emergence mitigation is that while spillover probability and  
240 initial ease of spread may be lower, so too is detection probability (41), because of the distance to  
241 healthcare. This may allow localized, remote outbreaks to establish and spread in human populations  
242 before detection (44-46). Our findings can be helpful in allocating efforts for surveillance,  
243 sustainability and conservation actions and long term plans for ecological intervention, including in  
244 areas with high emergent risk scores. Importantly, additional layers of prioritisation could be added to  
245 implement mitigation actions on hotspots, for instance, where climate change vulnerability is also  
246 high, such as in Java (47). Also, regions of China, in terms of mobility are outstandingly connected,  
247 which highlights the need to reduce pressures arising from multiple hotspots.

248 Scenario 2 (indirect transmission through livestock) had the highest number of regions with  
249 high-risk areas close to healthcare (yellow, Figure 4). These areas are extensive across the study  
250 region in all scenarios, and should be prioritised for temporal screening for viruses in livestock, the  
251 understanding of known hosts, and investments in improving public health responses to spread. High-  
252 risk areas far from healthcare (red) represent small regions of our study area (<1%) in all scenarios,  
253 where Scenario 1 had the fewest and Scenario 3 had the highest areas. These are areas with higher  
254 possibilities for spillover, that would also be likely to go undetected during the early stages of human-  
255 to-human transmission and spread. In those regions, urgent action to prevent contact, reduce  
256 deforestation, and enhance biodiversity protection should take place, as well as improvements in  
257 healthcare access. Human populations that are more vulnerable to risks could be targets for equitable  
258 distribution of promising solutions, such as pan-coronavirus vaccines (48).

259 Our findings are a snapshot of macroscale spatial trends that can be used for prioritising more  
260 detailed analysis depending on the context and policy priorities. The United Nations Development  
261 Programme (UNDP) recommends the creation of ‘Maps of Hope’ for maintaining essential life  
262 support areas (49), but the relationship between biodiversity loss, fragmentation, and zoonotic disease  
263 is seldom considered in the designation of such areas. We advocate for a One Health approach (50) in  
264 which the risks of pathogen emergence are explicitly integrated into initiatives addressing habitat  
265 management, restoration and protection (49), and have demonstrated that this risk can be mapped at  
266 large scales with insights into variability in the distribution of key drivers (50).

267 *Limitations*

268 We acknowledge the complexity of pathogen responses to land use modification (9), and  
269 important data use limitations for specific contexts. The static datasets used here are all global yet  
270 accessible. But hotspots may change in response to changes in economic and agricultural policies at  
271 national and subnational levels, international agreements such as Agenda 2030, and climate change  
272 adaptation (51). There are also several data limitations. Cryptic diversity in bats (52) and uneven  
273 sampling occur for sarbecoviruses and their bat hosts (15) create uncertainty regarding bats that is  
274 difficult to account for. Ecological analyses at finer spatial and temporal scales than used here can  
275 elucidate cascading events that result in zoonotic spillover. For example, Hendra virus spillover from  
276 bats to horses in Australia seems to be driven by interactions between climatic change altering the  
277 flowering phenology of important nectar sources, exacerbating food shortages resulting from native  
278 habitat loss and degradation, and nutritional stress in bats that can increase Hendra virus shedding.  
279 Native resource declines have concurrently promoted urbanization of many bat populations,  
280 increasing the human-bat interface and potential for spillover events to horses, which can act as  
281 intermediary hosts, or even potentially direct to humans (53). Our analyses may capture the  
282 macroscale processes, but not these local events.

283 Similarly, while knowing that the top-priority traded mammals (54) are correlated with total  
284 mammalian diversity, local analyses should evaluate factors that cannot be easily mapped or tracked,  
285 such as animal trade and hunting, which is currently not feasible using a macroscale approach. Our  
286 workflow can, however, be easily coupled with detailed local data for spillover ‘barriers’ and host  
287 characteristics to bring insights and customize action plans, such as data on reservoir density,  
288 pathogen prevalence, pathogen shedding, and data on spillover recipients, such as susceptibility and  
289 infection (55). This is especially important when macroscale and subnational level risk assessments  
290 are neither complete or validated for most nations (accessed in September 2022,  
291 <https://drmkc.jrc.ec.europa.eu/inform-index/INFORM-Subnational-Risk>).

292 The role of domestic intermediate hosts for sarbecoviruses is unclear, with numerous species  
293 able to be infected by SARS-CoV-2 (56). Here we include cattle and all Bovidae livestock  
294 evaluations, leading to similar overall results for clusters but with some univariate hotspots less  
295 intense, especially in central India and south China, while making them more intense around Beijing,  
296 highlighting how uncertainties around host susceptibility and potential pathways leads to uncertainty  
297 regarding risk. The emergence of a novel coronavirus and re-emergence of a known *Sarbecovirus*  
298 through spillback is also possible (56) and may change risk profiles. Other factors that play a large  
299 role in outbreak response such as conflict (57) and other societal challenges associated with health and  
300 the environment might also be considered.

301 *Conclusions*

302 The use of remote sensing layers can bring insights for land use planning when considering  
303 complex processes such as disease emergence. This process may benefit not only the understanding of  
304 risks but also local actions informed by broad patterns (28). Recent models suggest that the  
305 implementation of smaller-scale land-use planning strategies guided by macro-scale patterns may help  
306 to reduce the overall burden from emerging infectious diseases (58), while also taking into account  
307 biodiversity conservation. This could be evaluated from multiple perspectives, including in the  
308 context of other planetary boundaries and how zoonotic disease risk inserts within it (59), considering  
309 we have already passed the 1-degree warmer planet threshold (60).

310 This work contributes to strengthening evidence of transboundary clusters of risk factors for  
311 disease emergence. We use a reproducible workflow based on hotspot analysis from broad-scale data  
312 that is accessible through open software and maps for easy interpretation. This can enable local and  
313 national agencies to engage in new land-use planning actions by including stakeholders (academia,  
314 government, local communities and non-governmental organisations) under a One Health perspective.  
315 The need to reduce access to healthcare inequalities (61) without promoting encroachment into natural  
316 areas is a challenge. Efforts should focus on comprehensive land use planning on the place of  
317 healthcare facilities and other infrastructure (62). Biodiversity provides essential ecosystem services,  
318 so primary prevention of spillover can benefit sustainability at multiple scales, sustaining life on earth  
319 and human health (55). Our findings can help stakeholders when evaluating multiscale policies, land  
320 use planning and considering integrating community health programmes to universal healthcare  
321 implementation (63) into transboundary, national or subnational levels.

322 **Materials and Methods**

323 We use South, East and Southeast Asia (including West Papua) as our study region, where  
324 most *Sarbecovirus* hosts are concentrated (15, 16) and where many unknown sarbecoviruses are  
325 estimated to exist (29). We define our study region as the terrestrial area of the following countries:

326 Bangladesh, Bhutan, Brunei, Cambodia, China, India, Indonesia, Laos, Malaysia, Myanmar, Nepal,  
327 Philippines, Singapore, Sri Lanka, Thailand, Timor-Leste, and Vietnam.

328 *Characterization of univariate risk indicator hotspots*

329 We identified spatial clusters of components of risk. Our rationale for including each indicator  
330 relating to a SARS-like disease is presented in Table S1. We assume our inferred risk arises not from  
331 individual factors having outstanding high values (hotspots), but instead it arises when they are  
332 combined, facilitating conditions for viral spillover. In that sense our inference of risk is an emergent  
333 property of the system (Emergent risk). We adapted a broad-scale risk estimation framework  
334 (<https://mcr2030.undrr.org/quick-risk-estimation-tool>) focusing on the potential for sarbecoviruses to  
335 emerge. The broad risk factors were five landscape-level conditions and five biological layers,  
336 according to four scenarios (Table S1). The analysis is naive about the influence of individual drivers  
337 on the risk of spillover in the sense that all factors were weighted equally in our scenario evaluations.  
338 We selected the following factors for land use change and landscape conditions: Intensity of 1) built-  
339 up land, 2) mining and energy, 3) agricultural and harvest land, 4) forest quality, and 5) local forest  
340 loss risk. As a measure of human or animal exposure, we used livestock (pigs and cattle), wildlife  
341 (known bat hosts and all other wild mammals), and human populations. To avoid collinearity, we only  
342 selected variables with product-moment correlation coefficient ( $r$ ) values  $< \pm 0.7$  (Figure S1). There  
343 are many countries in Southeast Asia where carabao (*Bubalus bubalis*) and other Bovidae livestock  
344 are more common than cattle (*Bos taurus*) so we provide results for Bovidae livestock instead of  
345 cattle-only in the Supplementary materials.

346 The study region was divided into a spatial grid composed of 0.25 decimal degrees-sized tiles  
347 (~27 km). All indicators were resampled to match this resolution. For data layers that were counts  
348 from shapefiles (other mammal species numbers), we applied median values for resampling. We ran a  
349 univariate hotspot analysis based on Getis-ord G\* $i$  scores considering each factor individually at 95%  
350 alpha error cut-off. We created a list of closest neighbors considering all data and n=25 for the closest  
351 neighborhood. Local G assumes a two-sided alternative hypothesis, where high-positive values  
352 indicate hotspot regions and low negative values indicate coldspots. Pixels located in-between the  
353 alternative hotspot or coldspot hypothesis values are referred as intermediate regions, where the value  
354 may reflect random spatial process, i.e. no spatial clustering detected. Critical values for defining  
355 univariate hotspots followed the critical values for 95th percentile (64).

356 *Scenarios*

357 Detected hotspots for all landscape condition components were used in combination with  
358 biological components in the scenario analyses. Scenario 1 considers direct transmission from bats to  
359 humans, where the biological risk is composed of the average number of bat species in which

360 sarbecoviruses have been reported as the known primary hosts. For Scenario 2, we then considered  
361 the components of scenario one in combination with potential intermediate hosts using: pig counts,  
362 cattle-only or Bovidae livestock counts. Scenario 3 considered bat hosts and the number of other wild  
363 mammal species present. For Scenario 3, we used the wild mammals layer (minus known bat hosts)  
364 and known bat hosts as the potential intermediate hosts. We considered using a traded mammal layer  
365 instead of an all wild mammal layer in Scenario 3, because of evidence the first Covid-19 cases  
366 identified were linked to the Huanan Seafood Wholesale Market in Wuhan (18). An available high  
367 priority traded mammal layer (54), however, is highly correlated ( $r = 0.864$ ) with the wild mammal  
368 layer. Because of this correlation in addition to high uncertainty regarding trade, we kept only the  
369 mammal layer and bat hosts layer in Scenario 3. A fourth scenario including all of the previous  
370 mammalian layers, be it wild or livestock, was constructed. We plotted counts of hotspots  
371 (convergence of hotspots) and the differences between every scenario map and the map from Scenario  
372 1 (lowest number of variables, direct transmission), to help understand how much risk is added when  
373 we have other potential intermediate hosts to the system.

374 *Hotspot convergence in clusters*

375 We evaluated the spatial clustering among hotspots including all the selected indicators (Scenario 4,  
376 five landscape descriptors, five potential host components). We opted for doing a single cluster  
377 analysis because we cannot weigh the importance of the single variables for influencing an ultimate  
378 spillover event. The variables comprised here describe landscape condition, human population, cattle,  
379 pig, bat hosts and all other wild mammals. We assume areas that contain most hotspots or that are on  
380 the verge of becoming hotpots (intermediate areas) for the components evaluated are at higher risk of  
381 emerging new sarbecoviruses. A multivariate spatial cluster analysis was applied to scores for every  
382 variable after the univariate hotspot analysis using rgeoda 0.0.9 (65). We used the multivariate skater  
383 (Spatial `K'luster Analysis by Tree Edge Removal) hierarchical partitioning algorithm (66) to infer  
384 contiguous clusters of similar values in the region based on the optimal pruning of a minimum  
385 spanning tree. Spatial clusters represent emergent, cohesive risk combinations distributed in space.  
386 Contiguity was assessed by a queen weights matrix after transforming pixels to geographical  
387 coordinates. Distance functions were set to euclidean. We evaluated the k number of clusters from 1  
388 to 40. To find the optimal number of clusters, we evaluated the total within-cluster sum of squares  
389 variation, visually inspecting the point of inflection in the curve towards stabilization. As the  
390 reduction in increment was very smooth, we present the number of clusters for skater informed by the  
391 max-p algorithm. We used max-p to find the solution for the optimal number of spatially-defined  
392 clusters setting as a bounding variable (a variable that allows for a minimum value summed for each  
393 cluster) the human population amounts at 5% and 10%. The algorithm was computed at 99 interactions  
394 with 123456789 as a random seed.

395 To interpret variation of hotspots within clusters, we counted the number of variables for which the  
396 median of the value distribution is a hotspot (i.e. falling within the hotspot interval at 95% Gi\*). We  
397 then discuss the clusters based on the number of indicators that are already hotspots and the  
398 distribution that falls in intermediate zones, so closer to becoming hotspots, which may be ones  
399 contributing to greater spillover risk in the near future. We did this by evaluating the density  
400 distribution of variables in a ridgeline plot. Finally, to understand the overall variation (and among  
401 clusters) we provide a Principal component analysis (PCA) biplot through Scenario 4 to discuss major  
402 axes of variation between optimal number of clusters. We ran the hotspot analyses with cattle-only  
403 and with the summed values for Bovidae livestock (presented in the Supplemental Material). All  
404 geographical coordinates were warped to World Mercator (EPSG: 3395) and World Geodetic System  
405 1984 datum before spatial analysis.

406 *Emergent risk and its relationship with access to healthcare*

407 After identifying the hotspots within the scenarios, we match their proximity to detection by matching  
408 their information with the level of motorized access to healthcare. Access to healthcare measured as  
409 travel time was considered as both a proxy for connectivity and an indicator of the likelihood of  
410 detection, following infection spillover and spread. We built bivariate maps and three-by-three  
411 quantile (N=9) combinations considering the intensity of hotspots from their overlay scaled and scaled  
412 values for access to healthcare, all rescaled from zero to one. All analyses were done in QGIS 3.10.7  
413 (67), R 4.1.3 (68) and bash (69). Code for the analyses can be found at  
414 <https://github.com/renatamuy/hotspots/>.

415

416 **References and notes**

- 417 1. N. D. Wolfe, C. P. Dunavan, J. Diamond, Origins of major human infectious diseases. *Nature*.  
418 **447**, 279–283 (2007).
- 419 2. A. Düx, S. Lequime, L. V. Patrono, B. Vrancken, S. Boral, J. F. Gogarten, A. Hilbig, D. Horst,  
420 K. Merkel, B. Prepoint, S. Santibanez, J. Schlotterbeck, M. A. Suchard, M. Ulrich, N. Widulin,  
421 A. Mankertz, F. H. Leendertz, K. Harper, T. Schnalke, P. Lemey, S. Calvignac-Spencer, Measles  
422 virus and rinderpest virus divergence dated to the sixth century BCE. *Science*. **368**, 1367–1370  
(2020).
- 424 3. R. Antia, R. R. Regoes, J. C. Koella, C. T. Bergstrom, The role of evolution in the emergence of  
425 infectious diseases. *Nature*. **426**, 658–661 (2003).
- 426 4. J. O. Lloyd-Smith, D. George, K. M. Pepin, V. E. Pitzer, J. R. C. Pulliam, A. P. Dobson, P. J.  
427 Hudson, B. T. Grenfell, Epidemic dynamics at the human-animal interface. *Science*. **326**, 1362–  
428 1367 (2009).
- 429 5. R. K. Plowright, J. K. Reaser, H. Locke, S. J. Woodley, J. A. Patz, D. J. Becker, G. Oppler, P. J.  
430 Hudson, G. M. Tabor, Land use-induced spillover: a call to action to safeguard environmental,

431 animal, and human health. *Lancet Planet Health.* **5**, e237–e245 (2021).

432 6. M. C. Hansen, P. V. Potapov, A. H. Pickens, A. Tyukavina, A. Hernandez-Serna, V. Zalles, S.  
433 Turubanova, I. Kommareddy, S. V. Stehman, X.-P. Song, A. Kommareddy, Global land use  
434 extent and dispersion within natural land cover using Landsat data. *Environ. Res. Lett.* **17**,  
435 034050 (2022).

436 7. P. Eby, A. J. Peel, A. Hoegh, W. Madden, J. R. Giles, P. J. Hudson, R. K. Plowright, Pathogen  
437 spillover driven by rapid changes in bat ecology. *Nature* (2022), doi:10.1038/s41586-022-05506-  
438 2.

439 8. C. A. Sánchez, J. Venkatachalam-Vaz, J. M. Drake, Spillover of zoonotic pathogens: A review  
440 of reviews. *Zoonoses Public Health.* **68**, 563–577 (2021).

441 9. A. D. Mader, N. A. Waters, E. C. Kawazu, M. Marvier, N. Monnin, D. J. Salkeld, Messaging  
442 Should Reflect the Nuanced Relationship between Land Change and Zoonotic Disease Risk.  
443 *Bioscience*, biac075 (2022).

444 10. C. E. Snedden, S. K. Makanani, S. T. Schwartz, A. Gamble, R. V. Blakey, B. Borremans, S. K.  
445 Helman, L. Espericueta, A. Valencia, A. Endo, M. E. Alfaro, J. O. Lloyd-Smith, SARS-CoV-2:  
446 Cross-scale Insights from Ecology and Evolution. *Trends Microbiol.* **29**, 593–605 (2021).

447 11. J. K. Reaser, B. E. Hunt, M. Ruiz-Aravena, G. M. Tabor, J. A. Patz, D. J. Becker, H. Locke, P. J.  
448 Hudson, R. K. Plowright, Fostering landscape immunity to protect human health: A  
449 science-based rationale for shifting conservation policy paradigms. *Conserv. Lett.* (2022),  
450 doi:10.1111/conl.12869.

451 12. R. Gibb, D. W. Redding, K. Q. Chin, C. A. Donnelly, T. M. Blackburn, T. Newbold, K. E. Jones,  
452 Zoonotic host diversity increases in human-dominated ecosystems. *Nature.* **584**, 398–402 (2020).

453 13. S. Lytras, J. Hughes, D. Martin, P. Swanepoel, A. de Klerk, R. Lourens, S. L. Kosakovsky Pond,  
454 W. Xia, X. Jiang, D. L. Robertson, Exploring the Natural Origins of SARS-CoV-2 in the Light of  
455 Recombination. *Genome Biol. Evol.* **14** (2022), doi:10.1093/gbe/evac018.

456 14. A. Latinne, B. Hu, K. J. Olival, G. Zhu, L. Zhang, H. Li, A. A. Chmura, H. E. Field, C.  
457 Zambrana-Torrelío, J. H. Epstein, B. Li, W. Zhang, L.-F. Wang, Z.-L. Shi, P. Daszak, Origin and  
458 cross-species transmission of bat coronaviruses in China. *Nat. Commun.* **11**, 4235 (2020).

459 15. R. L. Muylaert, T. Kingston, J. Luo, M. H. Vancine, N. Galli, C. J. Carlson, R. S. John, M. C.  
460 Rulli, D. T. S. Hayman, Present and future distribution of bat hosts of sarbecoviruses:  
461 implications for conservation and public health. *Proc. Biol. Sci.* **289**, 20220397 (2022).

462 16. C. A. Sánchez, H. Li, K. L. Phelps, C. Zambrana-Torrelío, L.-F. Wang, P. Zhou, Z.-L. Shi, K. J.  
463 Olival, P. Daszak, A strategy to assess spillover risk of bat SARS-related coronaviruses in  
464 Southeast Asia. *Nat. Commun.* **13**, 4380 (2022).

465 17. World Health Organization, WHO-convened global study of origins of SARS-CoV-2: China  
466 part. *World Health Organization* (2021) (available at <https://apo.org.au/node/311637>).

467 18. M. Worobey, J. I. Levy, L. Malpica Serrano, A. Crits-Christoph, J. E. Pekar, S. A. Goldstein, A.  
468 L. Rasmussen, M. U. G. Kraemer, C. Newman, M. P. G. Koopmans, M. A. Suchard, J. O.  
469 Wertheim, P. Lemey, D. L. Robertson, R. F. Garry, E. C. Holmes, A. Rambaut, K. G. Andersen,  
470 The Huanan Seafood Wholesale Market in Wuhan was the early epicenter of the COVID-19  
471 pandemic. *Science.* **377**, 951–959 (2022).

472 19. L. Joffrin, A. O. G. Hoarau, E. Lagadec, O. Torrontegi, M. Köster, G. Le Minter, M. Dietrich, P.

473 474 Mavingui, C. Lebarbenchon, Seasonality of coronavirus shedding in tropical bats. *R Soc Open Sci.* **9**, 211600 (2022).

475 476 477 478 20. D. Montecino-Latorre, T. Goldstein, T. R. Kelly, D. J. Wolking, A. Kindunda, G. Kongo, S. O. Bel-Nono, R. R. Kazwala, R. D. Suu-Ire, C. M. Barker, C. K. Johnson, J. A. K. Mazet, Seasonal shedding of coronavirus by straw-colored fruit bats at urban roosts in Africa. *PLoS One.* **17**, e0274490 (2022).

479 480 481 482 21. S. Wacharapluesadee, P. Duengkae, A. Chaiyees, T. Kaewpom, A. Rodpan, S. Yingsakmongkon, S. Petcharat, P. Phengsakul, P. Maneeorn, T. Hemachudha, Longitudinal study of age-specific pattern of coronavirus infection in Lyle's flying fox (*Pteropus lylei*) in Thailand. *Virol. J.* **15**, 38 (2018).

483 484 485 22. A. Seltmann, V. M. Corman, A. Rasche, C. Drosten, G. Á. Czirják, H. Bernard, M. J. Struebig, C. C. Voigt, Seasonal Fluctuations of Astrovirus, But Not Coronavirus Shedding in Bats Inhabiting Human-Modified Tropical Forests. *Ecohealth.* **14**, 272–284 (2017).

486 487 488 489 490 23. M. Ruiz-Aravena, C. McKee, A. Gamble, T. Lunn, A. Morris, C. E. Snedden, C. K. Yinda, J. R. Port, D. W. Buchholz, Y. Y. Yeo, C. Faust, E. Jax, L. Dee, D. N. Jones, M. K. Kessler, C. Falvo, D. Crowley, N. Bharti, C. E. Brook, H. C. Aguilar, A. J. Peel, O. Restif, T. Schountz, C. R. Parrish, E. S. Gurley, J. O. Lloyd-Smith, P. J. Hudson, V. J. Munster, R. K. Plowright, Ecology, evolution and spillover of coronaviruses from bats. *Nat. Rev. Microbiol.* **20**, 299–314 (2022).

491 492 24. R. Djalante, R. Shaw, A. DeWit, Building resilience against biological hazards and pandemics: COVID-19 and its implications for the Sendai Framework. *Prog Disaster Sci.* **6**, 100080 (2020).

493 494 495 25. L. Pearson, M. Pelling, The UN Sendai Framework for Disaster Risk Reduction 2015–2030: Negotiation Process and Prospects for Science and Practice. *J. of Extr. Even.* **02**, 1571001 (2015).

496 497 26. M. Pretorius, W. Markotter, M. Keith, Assessing the extent of land-use change around important bat-inhabited caves. *BMC Zoology.* **6**, 1–12 (2021).

498 499 500 27. M. C. Rulli, P. D'Odorico, N. Galli, D. T. S. Hayman, Land-use change and the livestock revolution increase the risk of zoonotic coronavirus transmission from rhinolophid bats. *Nature Food.* **2**, 409–416 (2021).

501 502 503 28. D. A. Wilkinson, J. C. Marshall, N. P. French, D. T. S. Hayman, Habitat fragmentation, biodiversity loss and the risk of novel infectious disease emergence. *J. R. Soc. Interface* (2018), doi:10.1098/rsif.2018.0403.

504 505 506 29. S. J. Anthony, C. K. Johnson, D. J. Greig, S. Kramer, X. Che, H. Wells, A. L. Hicks, D. O. Joly, N. D. Wolfe, P. Daszak, W. Karesh, W. I. Lipkin, S. S. Morse, J. A. K. Mazet, T. Goldstein, Global patterns in coronavirus diversity. *Virus Evol.* **3**, vex012 (2017).

507 508 509 510 511 30. H. Heesterbeek, R. M. Anderson, V. Andreasen, S. Bansal, D. De Angelis, C. Dye, K. T. D. Eames, W. J. Edmunds, S. D. W. Frost, S. Funk, T. D. Hollingsworth, T. House, V. Isham, P. Klepac, J. Lessler, J. O. Lloyd-Smith, C. J. E. Metcalf, D. Mollison, L. Pellis, J. R. C. Pulliam, M. G. Roberts, C. Viboud, Isaac Newton Institute IDD Collaboration, Modeling infectious disease dynamics in the complex landscape of global health. *Science.* **347**, aaa4339 (2015).

512 513 514 515 516 31. Z. L. Grange, T. Goldstein, C. K. Johnson, S. Anthony, K. Gilardi, P. Daszak, K. J. Olival, T. O'Rourke, S. Murray, S. H. Olson, E. Togami, G. Vidal, Expert Panel, PREDICT Consortium, J. A. K. Mazet, University of Edinburgh Epigroup members those who wish to remain anonymous, Ranking the risk of animal-to-human spillover for newly discovered viruses. *Proc. Natl. Acad. Sci. U. S. A.* **118** (2021), doi:10.1073/pnas.2002324118.

517 32. H. Guo, A. Li, T.-Y. Dong, J. Su, Y.-L. Yao, Y. Zhu, Z.-L. Shi, M. Letko, ACE2-Independent  
518 Bat Sarbecovirus Entry and Replication in Human and Bat Cells. *MBio*, e0256622 (2022).

519 33. N. Wang, S.-Y. Li, X.-L. Yang, H.-M. Huang, Y.-J. Zhang, H. Guo, C.-M. Luo, M. Miller, G.  
520 Zhu, A. A. Chmura, E. Hagan, J.-H. Zhou, Y.-Z. Zhang, L.-F. Wang, P. Daszak, Z.-L. Shi,  
521 Serological Evidence of Bat SARS-Related Coronavirus Infection in Humans, China. *Virol. Sin.*  
522 **33**, 104–107 (2018).

523 34. C. J. Carlson, G. F. Albery, C. Merow, C. H. Trisos, C. M. Zipfel, E. A. Eskew, K. J. Olival, N.  
524 Ross, S. Bansal, Climate change increases cross-species viral transmission risk. *Nature*. **607**,  
525 555–562 (2022).

526 35. A. S. Bernstein, A. W. Ando, T. Loch-Temzelides, M. M. Vale, B. V. Li, H. Li, J. Busch, C. A.  
527 Chapman, M. Kinnaird, K. Nowak, M. C. Castro, C. Zambrana-Torreljo, J. A. Ahumada, L.  
528 Xiao, P. Roehrdanz, L. Kaufman, L. Hannah, P. Daszak, S. L. Pimm, A. P. Dobson, The costs  
529 and benefits of primary prevention of zoonotic pandemics. *Sci Adv.* **8**, eabl4183 (2022).

530 36. H. Li, E. Mendelsohn, C. Zong, W. Zhang, E. Hagan, N. Wang, S. Li, H. Yan, H. Huang, G.  
531 Zhu, N. Ross, A. Chmura, P. Terry, M. Fielder, M. Miller, Z. Shi, P. Daszak, Human-animal  
532 interactions and bat coronavirus spillover potential among rural residents in Southern China.  
533 *Biosaf Health*. **1**, 84–90 (2019).

534 37. G. F. Albery, D. J. Becker, L. Brierley, C. E. Brook, R. C. Christofferson, L. E. Cohen, T. A.  
535 Dallas, E. A. Eskew, A. Fagre, M. J. Farrell, E. Glennon, S. Guth, M. B. Joseph, N. Mollentze,  
536 B. A. Neely, T. Poisot, A. L. Rasmussen, S. J. Ryan, S. Seifert, A. R. Sjodin, E. M. Sorrell, C. J.  
537 Carlson, The science of the host-virus network. *Nat Microbiol*. **6**, 1483–1492 (2021).

538 38. Y. Lu, Y. Yang, B. Sun, J. Yuan, M. Yu, N. C. Stenseth, J. M. Bullock, M. Obersteiner, Spatial  
539 variation in biodiversity loss across China under multiple environmental stressors. *Sci Adv.* **6**  
540 (2020), doi:10.1126/sciadv.abd0952.

541 39. P. Jaureguierry, N. Titeux, M. Wiemers, D. E. Bowler, L. Coscieme, A. S. Golden, C. A.  
542 Guerra, U. Jacob, Y. Takahashi, J. Settele, S. Díaz, Z. Molnár, A. Purvis, The direct drivers of  
543 recent global anthropogenic biodiversity loss. *Sci Adv.* **8**, eabm9982 (2022).

544 40. G. T. Keusch, J. H. Amuasi, D. E. Anderson, P. Daszak, I. Eckerle, H. Field, M. Koopmans, S.  
545 K. Lam, C. G. Das Neves, M. Peiris, S. Perlman, S. Wacharapluesadee, S. Yadana, L. Saif,  
546 Pandemic origins and a One Health approach to preparedness and prevention: Solutions based on  
547 SARS-CoV-2 and other RNA viruses. *Proc. Natl. Acad. Sci. U. S. A.* **119**, e2202871119 (2022).

548 41. K. E. Jones, N. G. Patel, M. A. Levy, A. Storeygard, D. Balk, J. L. Gittleman, P. Daszak, Global  
549 trends in emerging infectious diseases. *Nature*. **451**, 990–993 (2008).

550 42. V. Guernier, M. E. Hochberg, J.-F. Guégan, Ecology Drives the Worldwide Distribution of  
551 Human Diseases. *PLoS Biol.* **2**, e141 (2004).

552 43. G. R. Winck, R. L. G. Raimundo, H. Fernandes-Ferreira, M. G. Bueno, P. S. D'Andrea, F. L.  
553 Rocha, G. L. T. Cruz, E. M. Vilar, M. Brandão, J. L. P. Cordeiro, C. S. Andreazzi,  
554 Socioecological vulnerability and the risk of zoonotic disease emergence in Brazil. *Sci Adv.* **8**,  
555 eabo5774 (2022).

556 44. J. R. Giles, D. A. T. Cummings, B. T. Grenfell, A. J. Tatem, E. zu Erbach-Schoenberg, C. J. E.  
557 Metcalf, A. Wesolowski, Trip duration drives shift in travel network structure with implications  
558 for the predictability of spatial disease spread. *PLoS Comput. Biol.* **17**, e1009127 (2021).

559 45. S. Riley, C. Fraser, C. A. Donnelly, A. C. Ghani, L. J. Abu-Raddad, A. J. Hedley, G. M. Leung,

560 L.-M. Ho, T.-H. Lam, T. Q. Thach, P. Chau, K.-P. Chan, S.-V. Lo, P.-Y. Leung, T. Tsang, W.  
561 Ho, K.-H. Lee, E. M. C. Lau, N. M. Ferguson, R. M. Anderson, Transmission dynamics of the  
562 etiological agent of SARS in Hong Kong: impact of public health interventions. *Science*. **300**,  
563 1961–1966 (2003).

564 46. R. Li, S. Pei, B. Chen, Y. Song, T. Zhang, W. Yang, J. Shaman, Substantial undocumented  
565 infection facilitates the rapid dissemination of novel coronavirus (SARS-CoV-2). *Science*. **368**,  
566 489–493 (2020).

567 47. R. Green, P. Scheelbeek, J. Bentham, S. Cuevas, P. Smith, A. D. Dangour, Growing health:  
568 global linkages between patterns of food supply, sustainability, and vulnerability to climate  
569 change. *The Lancet Planetary Health*. **6**, e901–e908 (2022).

570 48. E. Dolgin, Pan-coronavirus vaccine pipeline takes form. *Nat. Rev. Drug Discov.* **21**, 324–326  
571 (2022).

572 49. Maps of Hope – UN Biodiversity Lab, (available at <https://unbiodiversitylab.org/maps-of-hope/>).

573 50. One Health High-Level Expert Panel (OHHLEP), W. B. Adisasmoro, S. Almuhairi, C. B.  
574 Behravesh, P. Bilivogui, S. A. Bukachi, N. Casas, N. C. Becerra, D. F. Charron, A. Chaudhary, J.  
575 R. Ciacci Zanella, A. A. Cunningham, O. Dar, N. Debnath, B. Dungu, E. Farag, G. F. Gao, D. T.  
576 S. Hayman, M. Khaitsa, M. P. G. Koopmans, C. Machalaba, J. S. Mackenzie, W. Markotter, T.  
577 C. Mettenleiter, S. Morand, V. Smolenskiy, L. Zhou, One Health: A new definition for a  
578 sustainable and healthy future. *PLoS Pathog.* **18**, e1010537 (2022).

579 51. "Transforming our world: The 2030 agenda for sustainable development" in *A New Era in  
580 Global Health* (Springer Publishing Company, New York, NY, 2018;  
581 <https://sdgs.un.org/2030agenda>).

582 52. A. Chornelia, J. Lu, A. C. Hughes, How to Accurately Delineate Morphologically Conserved  
583 Taxa and Diagnose Their Phenotypic Disparities: Species Delimitation in Cryptic Rhinolophidae  
584 (Chiroptera). *Front. Ecol. Evol.* **0** (2022), doi:10.3389/fevo.2022.854509.

585 53. D. J. Becker, A. D. Washburne, C. L. Faust, E. A. Mordecai, R. K. Plowright, The problem of  
586 scale in the prediction and management of pathogen spillover. *Philos. Trans. R. Soc. Lond. B  
587 Biol. Sci.* **374**, 20190224 (2019).

588 54. M. R. Cronin, L. A. de Wit, L. Martínez-Estevez, Aligning conservation and public health goals  
589 to tackle unsustainable trade of mammals. *Conservation Science and Practice*. **n/a**, e12818  
590 (2022).

591 55. Ecological interventions to prevent and manage zoonotic pathogen spillover, ,  
592 doi:10.1098/rstb.2018.0342.

593 56. A. Nerpel, L. Yang, J. Sorger, A. Käsbohrer, C. Walzer, A. Desvars-Larrive, SARS-ANI: a  
594 global open access dataset of reported SARS-CoV-2 events in animals. *Scientific Data*. **9**, 1–13  
595 (2022).

596 57. M. Gayer, D. Legros, P. Formenty, M. A. Connolly, Conflict and emerging infectious diseases.  
597 *Emerg. Infect. Dis.* **13**, 1625–1631 (2007).

598 58. R. E. Baker, A. S. Mahmud, I. F. Miller, M. Rajeev, F. Rasambainarivo, B. L. Rice, S.  
599 Takahashi, A. J. Tatem, C. E. Wagner, L.-F. Wang, A. Wesolowski, C. J. E. Metcalf, Infectious  
600 disease in an era of global change. *Nat. Rev. Microbiol.* **20**, 193–205 (2022).

601 59. J. Rockström, W. Steffen, K. Noone, Å. Persson, F. S. Chapin, E. F. Lambin, T. M. Lenton, M.

602 Scheffer, C. Folke, H. J. Schellnhuber, B. Nykvist, C. A. de Wit, T. Hughes, S. van der Leeuw,  
603 H. Rodhe, S. Sörlin, P. K. Snyder, R. Costanza, U. Svedin, M. Falkenmark, L. Karlberg, R. W.  
604 Corell, V. J. Fabry, J. Hansen, B. Walker, D. Liverman, K. Richardson, P. Crutzen, J. A. Foley,  
605 A safe operating space for humanity. *Nature*. **461**, 472–475 (2009).

606 60. D. I. Armstrong McKay, A. Staal, J. F. Abrams, R. Winkelmann, B. Sakschewski, S. Loriani, I.  
607 Fetzer, S. E. Cornell, J. Rockström, T. M. Lenton, Exceeding 1.5°C global warming could trigger  
608 multiple climate tipping points. *Science*. **377**, eabn7950 (2022).

609 61. Z. Tao, Q. Wang, Facility or Transport Inequality? Decomposing Healthcare Accessibility  
610 Inequality in Shenzhen, China. *Int. J. Environ. Res. Public Health*. **19** (2022),  
611 doi:10.3390/ijerph19116897.

612 62. K. B. Toh, J. Millar, P. Psychas, B. Abuaku, C. Ahorlu, S. Oppong, K. Koram, D. Valle, Guiding  
613 placement of health facilities using multiple malaria criteria and an interactive tool. *Malar. J.* **20**,  
614 455 (2021).

615 63. A. Gachitorena, F. A. Ihantamalala, C. Révillion, L. F. Cordier, M. Randriamihaja, B.  
616 Razafinjato, F. H. Rafenoarivamalala, K. E. Finnegan, J. C. Andrianirarison, J. Rakotonirina,  
617 V. Herbreteau, M. H. Bonds, Geographic barriers to achieving universal health coverage:  
618 evidence from rural Madagascar. *Health Policy Plan*. **36**, 1659–1670 (2021).

619 64. J. K. Ord, A. Getis, Local spatial autocorrelation statistics: Distributional issues and an  
620 application. *Geogr. Anal.* **27**, 286–306 (2010).

621 65. X. Li, L. Anselin, rgeoda: R Library for Spatial Data Analysis (2022).

622 66. R. M. Assunção, M. C. Neves, G. Câmara, C. Da Costa Freitas, Efficient regionalization  
623 techniques for socio-economic geographical units using minimum spanning trees. *Int. J. Geogr.  
624 Inf. Sci.* **20**, 797–811 (2006).

625 67. QGIS Development Team, *QGIS Geographic Information System* (Open Source Geospatial  
626 Foundation, 2009; <http://qgis.osgeo.org>).

627 68. R Core Team, R: A Language and Environment for Statistical Computing (2020), (available at  
628 <https://www.R-project.org/>).

629 69. P. Gnu, Free Software Foundation. *Bash (3. 2. 48)[Unix shell program]*.

### 630 **Acknowledgments**

631 We thank Dr Jinhong Luo for comments on an earlier version of the draft. Massey University's  
632 subscription to New Zealand eScience Infrastructure (NeSi) enabled us to use high-performance  
633 computing facilities. Te Pūnaha Matatini gave us support during the 2022 Mahia Te Mahi workshop.

### 634 **Funding**

635 RLM, DTS, RSJ: Bryce Carmine and Anne Carmine (née Percival), through the Massey University  
636 Foundation; DTS: Royal Society Te Apārangi, grant number MAU1701.

### 637 **Competing interests**

638 The authors declare that they have no competing interests.

639

640 **Competing interests**

641 All data needed to evaluate the conclusions in the paper are present in the paper and the  
642 Supplementary Materials.

643